Braz J Phys (2014) 44:45–54
DOI 10.1007/s13538-013-0166-6

CONDENSED MATTER

Diffusion Mechanism in Liquid MgO: Insights from Simulation

N. V. Hong · M. T. Lan · P. K. Hung

Received: 15 November 2012 / Published online: 4 December 2013

Abstract A molecular dynamics study of the microstructure and of diffusion in liquid MgO is reported. Models with 2,000 atoms were constructed in a wide temperature range, from 3,400 to 5,000 K, at ambient pressure. Analyses of the nearest-neighbor atomic exchange among coordination units, lifetime of the coordination units, temperature dependence of the velocity of the $MgO_x \rightarrow MgO_{x\pm1}$ transitions, and dependence of the mean-squared displacement on the number of transitions provide information on the structural dynamics and diffusion mechanism. A new method to calculate the diffusion coefficients is proposed, which yields coefficients in agreement with the Einstein equation, a result that sheds light on the mechanism of diffusion in liquid MgO. The dynamics is shown to be spatially heterogeneous and the origin of this heterogeneity is identified.

Keywords Microstructure · Dynamics · Transition · Diffusion Mechanism

1 Introduction

Most liquids, including oxides, alloys, polymeric liquids, and many others form a metastable supercooled state if cooled fast enough to avoid crystallization. The dynamical behavior of glass-forming liquids exhibit many interesting features, such as non-exponential, multi-stage decay of fluctuations, absence of changes in static structural quantities, and rapidly increasing relaxation times [1–4]. Numerous approaches and several theories have been proposed to explain these behaviors [5–7]. The Adam–Gibbs approach [8, 9] is fundamentally based on the concept of cooperatively rearranging regions (CRRs), under the assumptions that the CRRs are independent of each other and contain a number of atoms sufficiently large to validate the methods of statistical mechanics. The Adam–Gibbs theory connects dynamics to thermodynamics and rationalizes the Vogel–Fulcher law, but the validity of its assumptions is still under debate.

A free volume theory of the glass transition was put forward by Cohen and Turnbull [10–12], who proposed that the neighborhood of an atom cannot be changed unless a free nearby volume can be found. The atoms diffuse through the local free volume. Although the theory offers good agreement with the Vogel–Fulcher–Tamman law, the free volume concept is not well-defined, and the pressure dependence of the viscosity is inadequately accounted for. Besides, the free volume vanishes at nonzero temperatures, a finding that has not yet been clarified. Another formulation regarding the glass transition as a density-fluctuation process is the Mode Coupling Theory (MCT) [13–15]. The MCT well describes many aspects of supercooled liquids, but it predicts dynamical arrest and the system to turn into a glass at a temperature T_{MCT} that exceeds the experimental Tg. Goldstein [16] argued that below T_{MCT}, the atomic motion is dominated by potential energy barriers that are high in comparison with the thermal energies, and the slow relaxation is due to thermally activated processes taking the system from one potential energy minimum to another.

On the basis of Goldstein's free-energy landscape picture, Stillinger and others [17–24] proposed the concept of inherent structure. The inherent structure formalism is capable of interpreting many observations in liquids and glasses, but it has not yet identified the physical mechanism responsible for the slowing down of supercooled liquids. The dynamical behavior of glass-forming liquids can be rationalized in another way, given the by now well-established existence of dynamical heterogeneity, identified in experiments and computer simulations [4, 25–28]. In MD simulations, dynamical

N. V. Hong (✉) · M. T. Lan · P. K. Hung
Hanoi University of Science and Technology, No. 1, Dai Co Viet Road, Hanoi, Vietnam
e-mail: hong.nguyenvan@hust.edu.vn

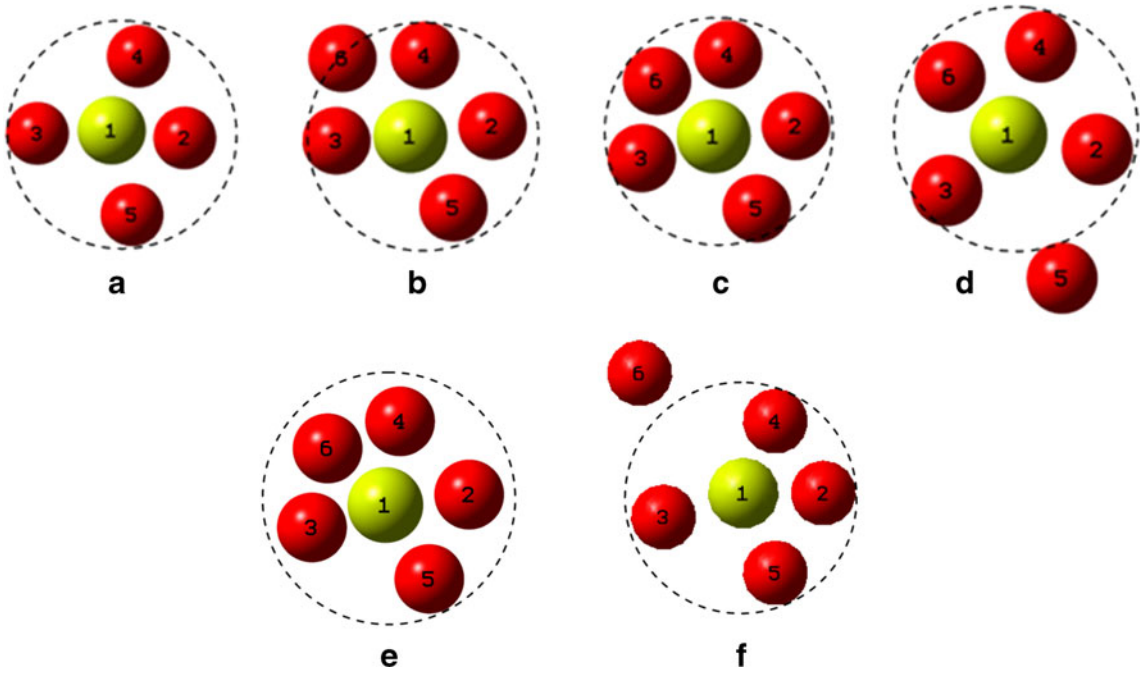

Fig. 1 Schematic depiction of diffusion in liquid MgO (colored online)

heterogeneities are usually characterized by the aggregations of the most mobile and of the least mobile atoms. The clustering of mobile atoms has been confirmed in 3D confocal microscopy experiments on colloidal suspension with liquid-like densities in the vicinity of Tg performed by Weeks and coworkers [29]. Clusters of mobile atoms are seen to grow and shrink with the observation time as atoms escape their cages and become trapped again, the cluster size increasing as T decreases [26]. Notwithstanding many decades of extensive experimental work, theoretical investigations, and simulations [5–15], no consensus has been reached concerning a complete theoretical description of the experimentally observed behavior of glass-forming liquids. In particular, the origin of the spatially heterogeneous dynamics remains mysterious.

Recently we gave detailed attention to the microstructural and dynamical properties of liquid MgO, a prototypical fragile-glass former, at pressures ranging from 0 to 25 GPa [30]. The results showed the structure of liquid MgO to consist of MgO_x structural units ($x=3, 4, 5, 6, 7$). Upon compression, the size of the units decreases slightly, but the shape is unchanged, independent of pressure. The results for dynamical properties showed that each atom undergoes a series of stages in which the structure of the coordination unit MgO_x or OMg_y to which it belongs is unchanged. The lifetime of the coordination units, as well as the transition rate, is strongly pressure dependent. We associated diffusion with the transitions, which lead to the nearest-neighbor atomic exchange among the coordination units MgO_x or OMg_y. The transition distribution showed the dynamics in liquid MgO to be spatially heterogeneous.

Here, we continue to investigate liquid MgO in a wide temperature range. We calculate and analyze the structural and dynamical properties, and the diffusion mechanism. We

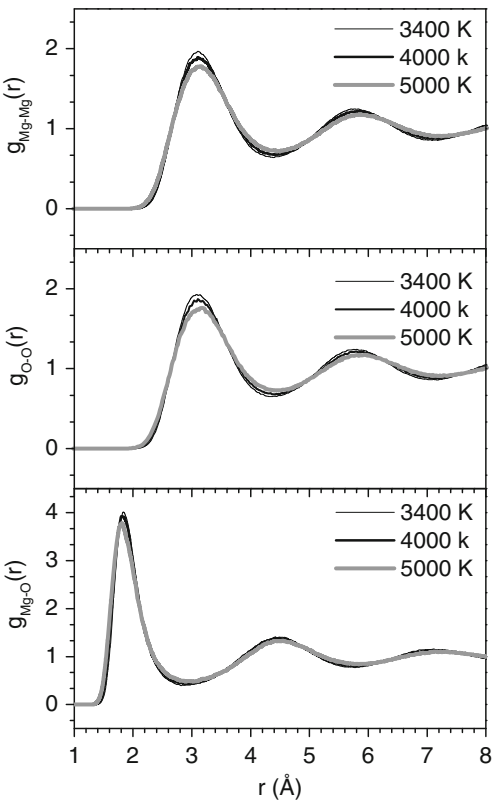

Fig. 2 Radial distribution functions of Mg–Mg, Mg–O, and O–O pairs at the indicated temperature

Table 1 Coordination distribution for liquid MgO at different temperatures

T (K)	3,400	3,600	3,800	4,000	4,200	4,500	5,000
C_2	0.42	0.39	0.68	0.84	1.1	1.89	1.94
C_3	18.37	18.81	20.33	20.6	21.02	21.66	22.86
C_4	54.76	53.9	52.57	51.35	51.06	49.57	47.35
C_5	23.24	23.29	23.4	23.82	23.52	23.69	24.15
C_6	2.65	2.71	2.78	2.81	2.85	2.94	3.15

C_x denotes the percent fraction of the MgO_x unit

propose a new approach, in which the dynamical behavior of glass-forming liquids is viewed as the nearest-neighbor atomic exchange among coordination units. We compute the Mg diffusion coefficient in liquid MgO by two methods and compare the two results to describe the diffusion mechanism. In addition, we discuss the relation between the structure and the spatially heterogeneous dynamics.

2 Computational Procedure

Our MD simulation is carried out with MgO models consisting of 2,000 atoms; 1,000 magnesium; and 1,000 oxygen, with periodic boundary conditions. We use the Lewis–Catlow potential. More details about this potential can be found in Ref. [31]. We integrate the equation of motion with the Verlet algorithm, in 1.6 fs time steps. In the initial configuration, all atoms are randomly placed in a simulation box and heated up to 7,000 K to remove possible memory effects. The sample is subsequently cooled down to the desired temperature. Next, a long relaxation in ensemble NPT (at constant temperature and pressure) yields the equilibrium sample. Seven models have been constructed this way at ambient pressure and at temperatures ranging from 3,400 to 5,000 K. To study dynamical properties, the obtained samples are relaxed in ensemble NVE (at constant volume and energy). In order to improve statistics, the measured quantities such as coordination number and pair radial distribution function (PRDF) are computed by averaging over 1,000 configurations separated by 10 time steps.

MgO liquid at ambient pressure consists of the coordination units (basic structural units) MgO_x (x=2, 3, 4, 5, 6), which are connected to each other by bridging oxygen atoms and form a spatial network structure. The tetrahedral coordination units (MgO_4) are dominant, about 50 %, the remaining fraction comprising the other coordination units (MgO_2, MgO_3, MgO_5, MgO_6). The diffusion of Mg is obviously impossible unless coordinated oxygen atoms are exchanged among the MgO_x units. Figure 1 illustrates diffusion by exchange of coordinated oxygen atoms. Six sequential stages are shown: in Figure 1a, the initial MgO_4 consists of one Mg and four coordinated oxygen atoms labeled 2, 3, 4, and 5. Next, a $MgO_4 \rightarrow MgO_5$ transition occurs, i.e., oxygen atom 6 moves inside the unit and transforms the MgO_4 unit into MgO_5, which consists of an Mg and the five oxygen atoms 2, 3, 4, 5, and 6 (Fig. 1c). In the following step, a $MgO_5 \rightarrow MgO_4$ transition occurs, but in this case, atom 5 leaves the MgO_5 unit and a new MgO_4 unit comprising oxygen atoms 2, 3, 4, and 6 is created (Fig. 1d). Next, atom 5 returns, so that $MgO_4 \rightarrow MgO_5$ (Fig. 1e). Afterwards, atom 6 leaves the unit and $MgO_5 \rightarrow MgO_4$. The process therefore consists of four transition stages, two such that $MgO_4 \rightarrow MgO_5$ [Fig. 1a and c–e (here, Fig.1b is the transition between Fig. 1a and c)] and two with $MgO_5 \rightarrow MgO_4$ (Fig. 1c–f).

The stages in Fig. 1a and f are similar, both containing one magnesium and the four oxygen atoms 2, 3, 4, and 5. The stages in Fig. 1c and e are similar to each other. Hence, only three stages (Fig. 1a, c, and d) are different. We call these stages "non-repeated." Let $m_{s,i}$ and $m_{sn,i}$, with i denoting the i^{th} atom, be the number of all stages and non-repeated stages, respectively, that an Mg atom undergoes over a time interval of Δt. Obviously, $m_{sn,i} \leq m_{s,i}$. If many back-and-forth transitions occur, m_{sn} will be small, which reduces the mean-squared displacement (MSD). The diffusivity therefore depends not only on the transition rate $MgO_x \leftrightarrow MgO_{x+1}$, but also on the ratio $\eta_{sn\text{-}s}=M_{sn}/M_s$, where $M_s = \sum_{i=1}^{N} m_{s,i}$ and

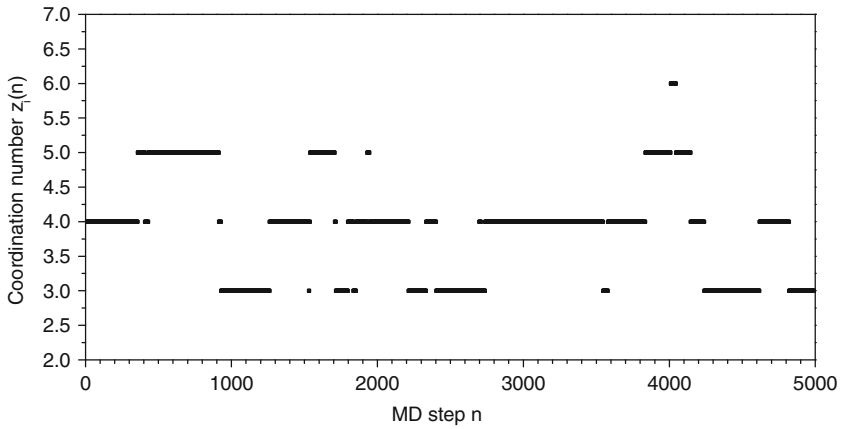

Fig. 3 Evolution of the coordination number $z_i(n)$ during 5,000 MD steps at 3,400 K temperature. $z_i(n)$ is the coordination number of the i^{th} atom at MD step n

Table 2 The variation of coordination number of the i^{th} Mg atom over stages

T (K)	Stage 1		Stage 2		Stage 3		Stage 4		Stag 5	
	Z_i	n_{step}	Z_i	n_{step}	Z_i	n_{step}	Z_i	n_{step}	Z_i	n_{step}
3,400	5	11	4	78	5	18	4	164	3	76
5,000	4	70	3	44	4	14	5	64	4	155

$M_{sn} = \sum_{i=1}^{N} m_{sn,i}$. Here, N is the total number of Mg atoms in the model. Let M_{tr} and $M_{NR\text{-}tr}$ be the number of transitions and non-repeated transitions of N magnesium atoms respectively. Since $M_{tr}=M_s-1$ and $M_{NR\text{-}tr}=M_{ns}-1$, we have $\eta_{sn\text{-}s}\cong M_{NR\text{-}tr}/M_{tr}$. In molecular dynamics simulations, the atomic diffusion coefficient is usually determined via the Einstein equation:

$$D = \lim_{t\to\infty} \frac{< r(t)^2 >}{6t} \tag{1}$$

Where $<r(t)^2>$ is the MSD over time t. If we define

$$D_{tr} = \lim_{m_{tr}\to\infty} \frac{< r(t)^2 >}{m_{tr}} \tag{2}$$

Equation (1) can be reduced to the form

$$D = \lim_{m_{tr}\to\infty} \frac{< r(t)^2 >}{6m_{tr}} \lim_{t\to\infty} \frac{m_{trans}}{t} = \frac{D_{tr}v_{tr}}{6.\Delta t} \tag{3}$$

where $t=n.\Delta t$; n is number of MD steps; Δt is MD step, equal to 1.6 fs; m_{tr} is the total number of MgO_x $MgO_{x\pm1}$ transitions per atom in n MD steps; and $m_{tr}=m_s-1$; $V_{tr}=m_{tr}/n$ is the rate of MgO_x $MgO_{x\pm1}$ transitions. To describe diffusion at the atomic level, we have calculated the diffusion coefficient by both methods, Eqs. (1) and (3).

Table 3 The lifetime distribution of MgO_x at different temperatures

T (K)	Average lifetime of MgO_x units, (MD step)						
	3,400	3,600	3,800	4,000	4,200	4,500	5,000
MgO_2	53.10	53.60	55.50	58.00	56.30	57.30	59.30
MgO_3	106.20	103.30	105.10	104.30	99.10	99.30	95.20
MgO_4	137.90	126.90	125.30	118.00	110.10	104.20	94.40
MgO_5	83.70	82.00	77.10	74.00	70.10	66.70	60.80
MgO_6	50.10	49.60	46.50	45.10	43.90	41.00	38.60

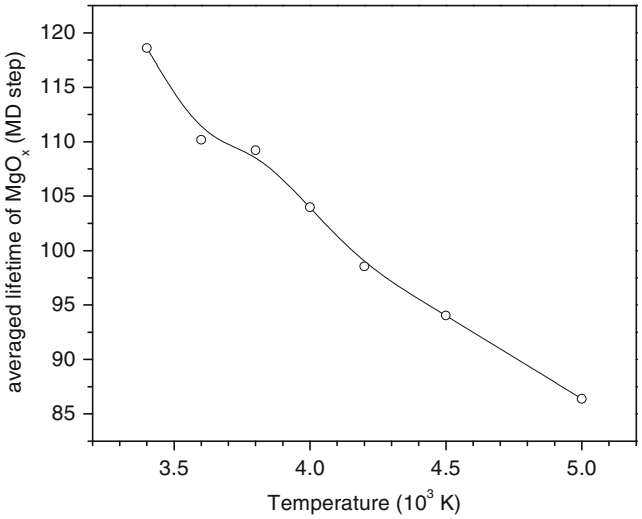

Fig. 4 Temperature dependence of the averaged lifetime of the MgO coordination units

3 Results and Discussion

3.1 Structural Properties

To ascertain that the constructed models are reliable, we have studied their characteristics. We have computed the PRDF's $g_{Mg-O}(r)$, $g_{Mg-Mg}(r)$, and $g_{O-O}(r)$ at different temperatures. Figure 2 shows the results at 3,400; 4,000; and 5,000 K. For all pairs (Mg–O, Mg–Mg, and O–O), the peak positions are nearly temperature-independent while the peak heights decrease slightly as the temperature rises. The RDF's $g_{Mg-Mg}(r)$ and $g_{O-O}(r)$ are similar to each other; with close to a 1 Å full-width half-maximum (FWHM). By contrast, the FWHM of the RDF $g_{Mg-O}(r)$ is rather small, nearly 0.5 Å. The first peaks of the PRDFs $g_{Mg-O}(r)$, $g_{Mg-Mg}(r)$, and $g_{O-O}(r)$ are located at 1.90, 3.10, and 3.12 Å, respectively. The

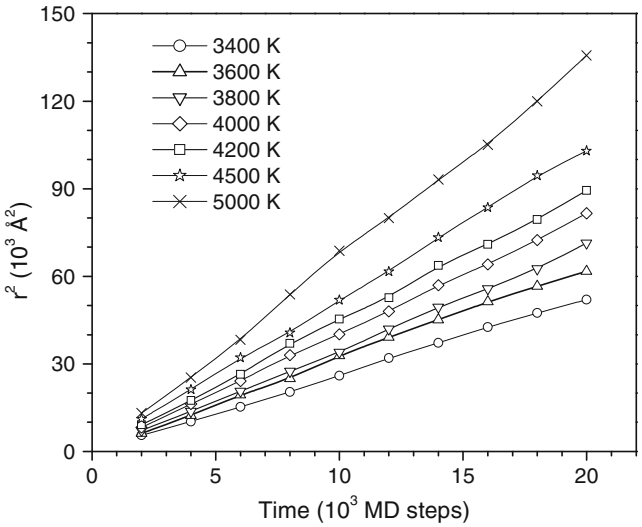

Fig. 5 Mean-squared displacement as a function of the number N of MD steps

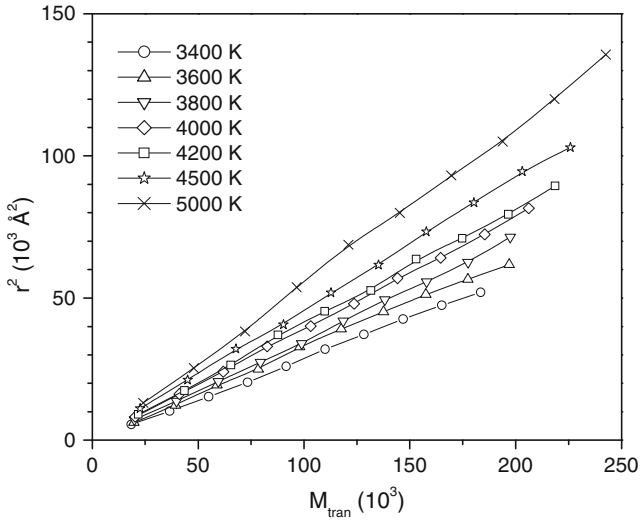

Fig. 6 Mean square displacement as a function of the number of transition M_{tran}

characteristics of the PRDFs are in good agreement with the calculated functions in [31–36] and the experimental data in [37, 38]. First-principles calculations and molecular dynamics simulations (for liquids MgO, $MgSiO_3$, and Mg_2SiO_4) show that the Mg–O bond length is between 1.92 and 1.97 Å. Neutron-diffraction experiment for the $MgSiO_3$ glass reveals an average Mg–O bond length of roughly 2.0 Å.

Table 1 shows the temperature dependence of the fraction of MgO_x (x=2–6) coordination units. In the displayed temperature range, from 3,400 to 5,000 K, the fraction of MgO_2 units is very small, less than 2 %. At 3,400 K, the distribution of Mg–O coordination numbers shows the following frequencies: 18.37 % MgO_3, 54.76 % MgO_4, 23.24 % MgO_5, and 2.65 % MgO_6. As the temperature rises, the fraction of MgO_4 units decreases slightly, from 54.76 % at 3,400 K to 47.35 % at 5,000 K. Conversely, the fractions of MgO_3 and MgO_6 units grow slightly. The fraction of MgO_5 units remains nearly unchanged as the temperature varies.

The average Mg–O coordination number is around 4.20 at 3,400 K, and 4.1 at 5,000 K. These results agrees with the first-principles calculations in [31, 33] and the experimental data in [36–38]. The first-principles calculations show that at ambient pressure, the average Mg–O coordination number is between 4.5 and 5 [33]. Neutron-diffraction data combined with x-ray diffraction data and a reverse Monte Carlo modeling for $MgSiO_3$ glass [37] show that the average Mg–O coordination number is close to 4.3, distributed among 61.9 % MgO_4, 33.2 % MgO_5, and 4.9 % MgO_6 sites, with a cutoff distance of 2.6 Å.

3.2 Dynamical Properties and Diffusion Mechanism

To describe diffusion at the atomic level, we trace the movement and change of coordination number for each atom during the simulation. Figure 3 shows the coordination number for one Mg atom along 5,000 MD steps at 3,400 K. Here $z_i(n)$ is the coordination number of the i^{th} atom at the n^{th} MD step n. Each atom goes through a series of stages, in each of which its coordination number remains fixed. Each stage occupies a time interval. In other words, a lifetime can be defined for each coordination unit. Most of the time, as Table 1 shows, the Mg atoms have coordination numbers 3, 4, and 5, corresponding to the coordination units MgO_3, MgO_4, and MgO_5. The lifetime of the tetrahedral coordination unit is the longest, i. e., the MgO_4 coordination unit is more stable than the others. Table 2 shows the coordination number of one Mg atom in a short interval, only five stages, corresponding to several

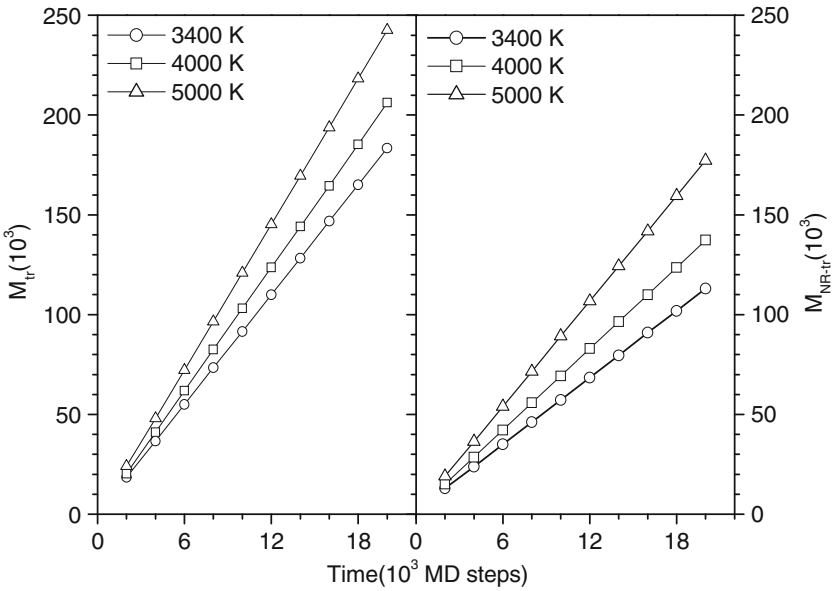

Fig. 7 Time dependence of the number of transitions (*left*) and number of non-repeated transitions (*right*)

Table 4 Dynamical characteristics of MgO liquids

T (K)	D_{tr} ($Å^2$/ *one* $MgO_x \rightarrow MgO_{x\pm1}$)	V_{tr}	$V_{NR\text{-}tr}$	$\eta_{sn\text{-}s}$	D (10^{-4} cm^2/s)
3,400	0.29	9.17	5.65	0.62	0.99
3,600	0.32	9.85	6.25	0.64	1.19
3,800	0.36	9.85	6.41	0.65	1.32
4,000	0.39	10.30	6.87	0.67	1.51
4,200	0.41	10.93	7.51	0.69	1.66
4,500	0.46	11.28	7.96	0.71	1.93
5,000	0.56	12.15	8.86	0.73	2.43

V_{tr} is the rate of $MgO_x \rightarrow MgO_{x\pm1}$ transitions, i.e., the number of $MgO_x \rightarrow MgO_{x\pm1}$ exchanges in one MD step; $V_{NR\text{-}tr}$ is the rate of non-repeated $MgO_x \rightarrow MgO_{x\pm1}$ transitions

hundreds of MD steps, extracted from the simulation. At 3,400 K, one Mg atom goes through five stages and takes the coordination numbers 5, 4, 5, 4, and 3, with lifetimes of 11, 78, 18, 164, and 76 MD steps, respectively. At 5,000 K, it goes through five stages, with coordination numbers 4, 3, 4, 5, and 4 and lifetimes of 70, 44, 14, 64, and 155 MD steps, respectively.

Table 3 shows the temperature-dependent lifetimes of the MgO_x coordination units. As the temperature rises, the lifetime of the MgO_2 coordination units grows from 53 MD steps (at 3,400 K) to 59 MD steps (at 5,000 K). By contrast, the lifetimes of other coordination units decrease. The lifetime of MgO_3, MgO_4, MgO_5, and MgO_6 decreases from 106.02, 137.90, 83.70, and 50.10 MD steps (at 3,400 K) to 95.20, 94.40, 60.80, and 38.60 MD steps (at 5,000 K) respectively. The average lifetime of MgO_x therefore decreases from roughly 118 MD steps (at 3,400 K) to 85 MD steps (at 5,000 K), as shown by Fig. 4. The coordination units of liquid MgO are therefore more stable at low temperature, an indication that as the temperature rises, the nearest-neighbor atomic exchange among coordination units becomes more frequent, which increases the diffusion coefficient. This diffusion mechanism is illustrated in Fig. 1. The MgO_4 unit initially consists of one Mg atom, numbered 1, and four oxygen atoms, labeled 2, 3, 4, and 5, as depicted in Fig. 1a. An outside oxygen atom, labeled 6, hops inside the MgO_4 unit to build the MgO_5 unit, as in Fig. 1b and c. As one of the neighbors of the Mg atom in the MgO_5 unit moves out, a new MgO_4 unit is formed, as in Fig. 1d. If this atom is the one labeled 6, i.e., the last one to hop in, the back-and-forth movements make no contribution to diffusion. In Fig. 1d, by contrast, the outward moving atom is the one labeled 5; the resulting movement does contribute to diffusion. To sum up, the nearest-neighbor exchange sequence a→b→c→d in Fig. 1 contributes to diffusion, while the sequence a→b→e→f makes no contribution.

Figure 5 shows the time-dependent MSD in liquid MgO at different temperatures. The MSD grows linearly with the simulation time, or number of MD steps, and rises strongly with temperature. Figure 6 shows the dependence of the MSD on the number of transitions at different temperatures. Again,

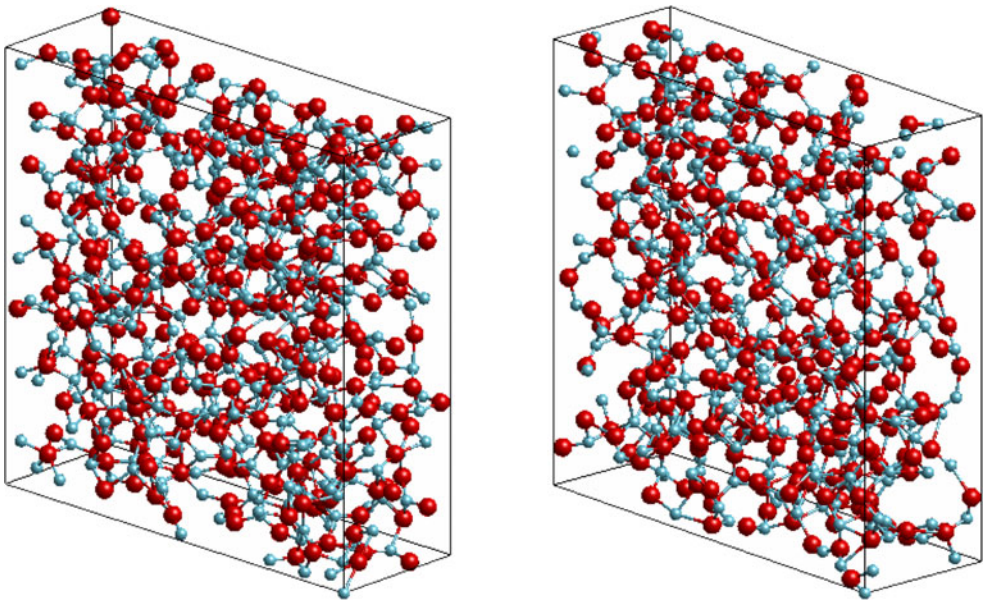

Fig. 8 Snapshot of the model liquid MgO at 3,400 K (*left*) and 5,000 K (*right*). The *small spheres* are O atom; the *other spheres* are Mg atoms (colored online)

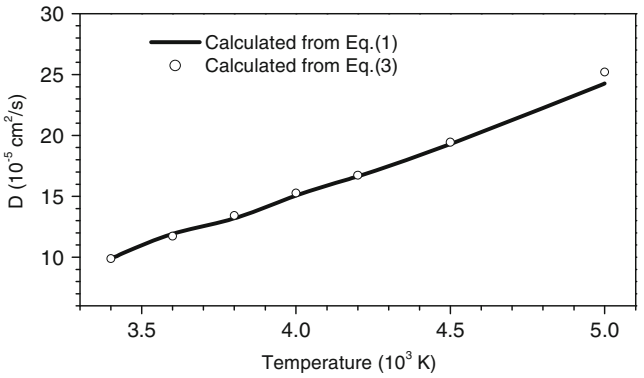

Fig. 9 Temperature dependence of diffusion coefficient of Mg in liquid MgO. The diffusion coefficient is calculate by two methods: calculation via Einstein equation (*solid line*) and calculation via the transitions $MgO_x \rightarrow MgO_{x\pm1}$ (*circles*)

the dependence is linear, once again demonstrating that diffusion in liquid MgO is due to nearest-neighbor atomic exchange among coordination units. The time dependences of the number of transitions M_{tr} and the number of non-repeated transitions $M_{NR\text{-}tr}$ are displayed in Fig. 7. Both M_{tr} and $M_{NR\text{-}tr}$ are linearly dependent on the simulation time. The linear fits in Figs. 6 and 7 yield the velocities V_{tr} and $V_{NR\text{-}tr}$, as well as the diffusion coefficient D_{tr}.

Table 4 presents V_{tr}, $V_{NR\text{-}tr}$, $\eta_{sn\text{-}s}$, D_{tr}, and D at different temperatures. Both V_{tr} and $V_{NR\text{-}tr}$ monotonously increase with temperature, indicating that they are well correlated with the diffusivity, since $\eta_{sn\text{-}s}\, E\, M_{NR\text{-}tr}/M_{tr}$ implies $\eta_{sn\text{-}s}\, E\, V_{NR\text{-}tr}/V_{tr}$. Since $\eta_{sn\text{-}s}$ also increases monotonously with temperature, we see that $V_{NR\text{-}tr}$ grows with temperature more rapidly than V_{tr}.

Consider the motion of one Mg atom over a time interval Δt_1. The Mg atom initially has x coordinated oxygen atoms. If Δt_1 is not too long, x_0 (where $x > x_0$) among these oxygen atoms remain at the nearest-neighbor distance, i.e., x_0 oxygen atoms bond with Mg to build MgO_{x0}, and the $x - x_0$ others move away from the nearest-neighbor distance. The Mg and x_0 coordinated oxygen atoms move together as a particle. Hence, the Mg atom within the MgO_{x0} particle diffuses in the network structure of our model, as in Fig. 8. Since MgO_{x0} is large in comparison with a single Mg atom, the mobility of Mg in the MgO_{x0} particle is smaller than that of the single Mg atom in the considered time interval. In addition, the MgO_{x0} unit blocks the diffusion of the other particles (Mg, O, and MgO_x). Since $\eta_{sn\text{-}s}$ is directly related to the number of MgO_{x0} particles, the diffusivity significantly depends on both quantities, V_{tr} and $\eta_{sn\text{-}s}$. Figure 9 shows the temperature dependence of the diffusion coefficient calculated by two methods: (1) via the Einstein Eq. (1); (2) via the new approach, i.e., via the $MgO_x \rightarrow MgO_{x\pm1}$ transitions, as described by Eq. (3). The agreement between the open circles representing Eq. (3) and the solid line representing Eq. (1) validates our code.

At very high temperatures, the lifetime of MgO_x is very short, because the transition rate is very high, and several transitions make no contribution to diffusion. At 5,000 K, the diffusion coefficient from Eq. (3) is a little higher than the one from Eq. (1), but the difference is negligible. The diffusion coefficient is in good agreement with the first-principle calculation in [33], which shows that the diffusion coefficients of Mg in liquid MgO at 4,000 and 5,000 K are 1.7×10^{-4} and 2.7×10^{-4} cm^2/s, respectively. Reference [38] calculated the properties of molten magnesium oxide with the significant-structure theory of liquids. Diffusion coefficients of 2.37×10^{-4}, 3.04×10^{-4}, and 3.7×10^{-4} were obtained for Mg at 3,400; 3,600; and 3,800 K, respectively, 2 to 3 times higher than the diffusion coefficients in this work, depending on the temperature.

The diffusivity in MD simulations significantly depends on the employed force field [39]; first-principle calculations are more accurate. The diffusion coefficients of Mg in liquid MgO in this work are very close to the ones in [33], which attests to the accuracy of the Lewis–Catlow potential and reliability of

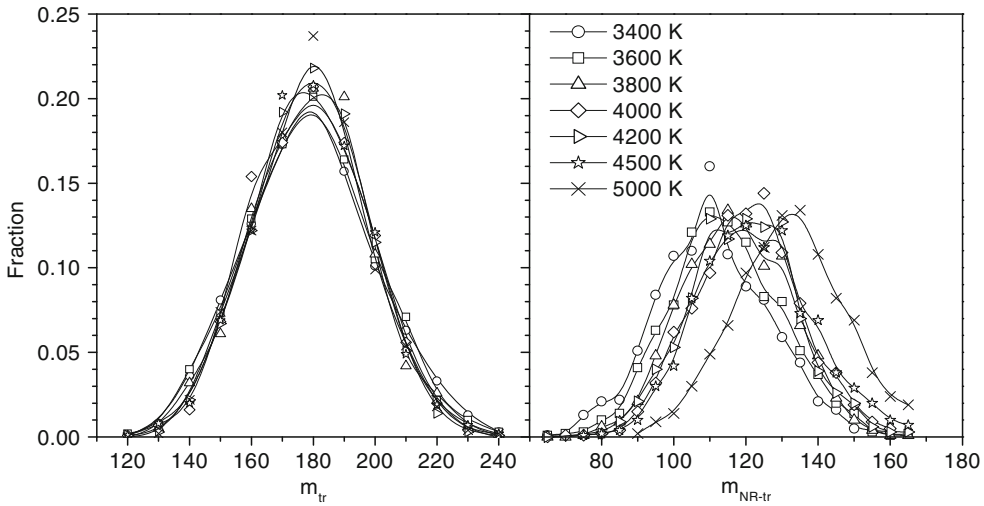

Fig. 10 Distribution of transitions (*left*) and non-repeated transition (*right*) for 20,000 MD step. Here, m_{tr} and $m_{NR\text{-}tr}$ are the number of transitions and non-repeated transitions, respectively, per Mg atom

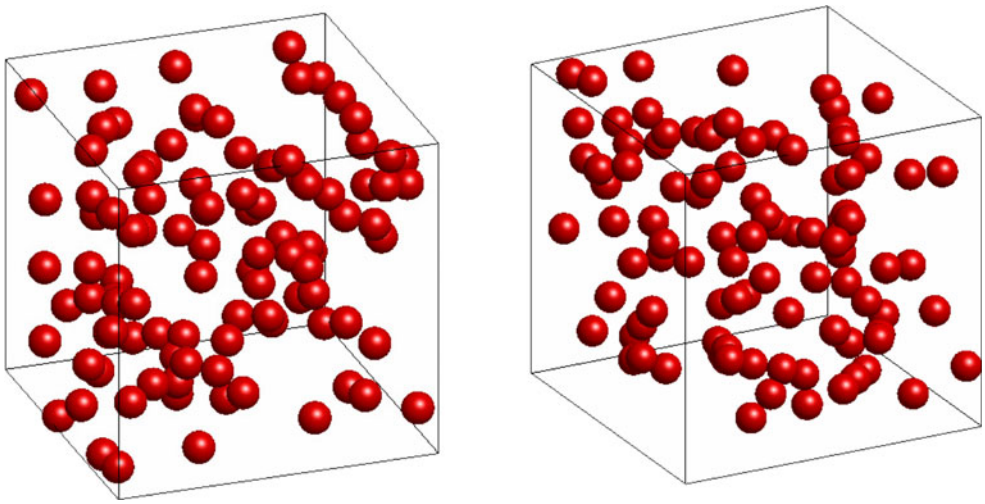

Fig. 11 Snapshot of the 100 atoms that are the most mobility in model liquid MgO at 3,400 K (*left*) and 5,000 K (*right*) (colored online)

calculated quantities. The diffusion coefficients calculated from Eqs. (1) and (3) indicate that diffusion in liquid MgO occurs via nearest-neighbor atomic exchange among coordination units. Because it is associated with the $MgO_x \rightarrow MgO_{x\pm1}$ transition, the diffusion will depend on the distribution of $MgO_x \rightarrow MgO_{x\pm1}$ transitions. Figure 10 shows the distribution of $MgO_x \rightarrow MgO_{x\pm1}$ transitions and non-repeated transitions around Mg atoms. Both distributions have Gaussian forms. For 20,000 MD steps, the average number of transitions per atom is close to 180. For the transition distribution, the shape, position of peak, and FWHM are nearly independent of temperature, but the peak height slightly increases as the temperature rises.

By contrast, the peak position for the non-repeated transition distribution systematically shifts to the right with increasing temperature, the average number of non-repeated transitions increasing from 110 at 3,400 K to 135 at 5,000 K. While the FWHM for the repeated transition is close to 60, the FWHM for the non-repeated transition distribution is close to 40 transitions. The large FWHM is evidence of spatially heterogeneous dynamics. From the distributions, it is clear that certain coordination units make very many transitions, from 220 to 240. Conversely, certain units make relatively few transitions, from 120 to 140 transitions. In the regions containing coordination units with higher than average number of transitions, i.e., higher than 180, the atoms are more mobile. Namely, the lifetimes of distinct MgO_x units ($x=3, 4, 5$) are different. The spatial distribution of the MgO_x units is not uniform; instead, for given x clusters of MgO_x are formed. The lifetime of the MgO_5 units is shorter than those of the other coordination units. The atoms in the MgO_5 clusters are more mobile than the ones in the MgO_3 or MgO_4 clusters. In the same time interval, the more mobile atoms undergo more transition than the others. The different widths of the transition distributions reflect the distinct mobilities of atoms at different locations. In other words, the most mobile atoms are sparse

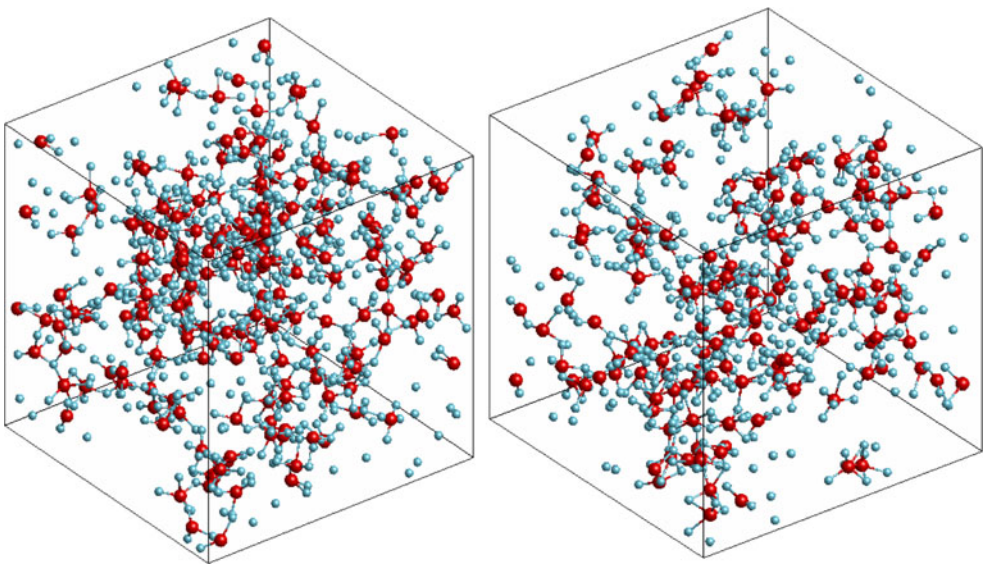

Fig. 12 Distribution of coordination units MgO_5 in liquid MgO at 3,400aK (*left*) and 5,000 K (*right*) (colored online)

and the dynamics is spatially heterogeneous. The more mobile atoms assist their neighbors to become more mobile. This is an example of dynamical facilitation, which forms mobile areas where the atoms are very mobile.

Figure 11 is a snapshot of the most mobile 100 atoms in the model liquid MgO at 3,400 K (left) and 5,000 K (right). The pictures confirm that the highly mobile atoms are not uniformly distributed in the model, but tend to cluster together, leading to spatially heterogeneous dynamics. Dynamical heterogeneity in liquids has been reported in Refs. [4, 25–29], but its origin was not identified. The lifetime of the MgO_5 coordination unit is the shortest among the lifetimes in Table 3. The mobility of an atom depends on its coordination unit. To understand the dynamical heterogeneity in liquid MgO, we have studied the distribution of the MgO_x units in model space.

Figure 12 displays the distribution of MgO_5 units, showing that the MgO_5 units tend to combine with each other to form clusters. Given that most of the coordination units in liquid MgO are MgO_x ($x=3, 4, 5$), Fig. 13 shows the temperature-dependent lifetimes of the MgO_3, MgO_4, and MgO_5 units. In the temperature range under study, the lifetime of MgO_5 is always much shorter than the lifetime of the two other types (MgO_3 and MgO_4). The atoms belonging to the MgO_5 units have high mobility, and the clusters of MgO_5 form mobile regions. Figure 14 shows the distribution of MgO_x ($x=3, 4, 5$) in the model of liquid MgO at 3,400 K. The regions with high mobility formed by the clustering of MgO_5 units are highlighted in red and the immobile regions formed by the clustering of the other unit types (MgO_3 and MgO_4) are painted black. The (red) mobile regions are occupying various regions, which are separated by (black) immobile regions. This interspersing of mobile and immobile regions constitutes spatially heterogeneous dynamics. To recapitulate, the distribution of MgO_5 units in the model is not uniform; instead, as Figs. 12 and 14 show, clusters are formed in such a way that structural heterogeneity arises and originates spatially heterogeneous dynamics.

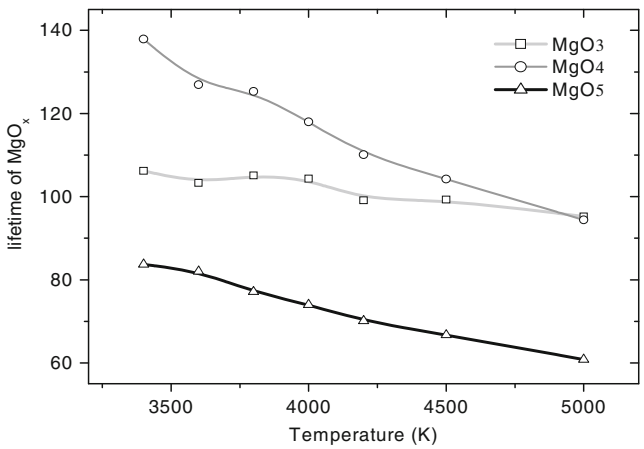

Fig. 13 The temperature dependence of lifetime of coordination units MgO_x ($x=3, 4, 5$)

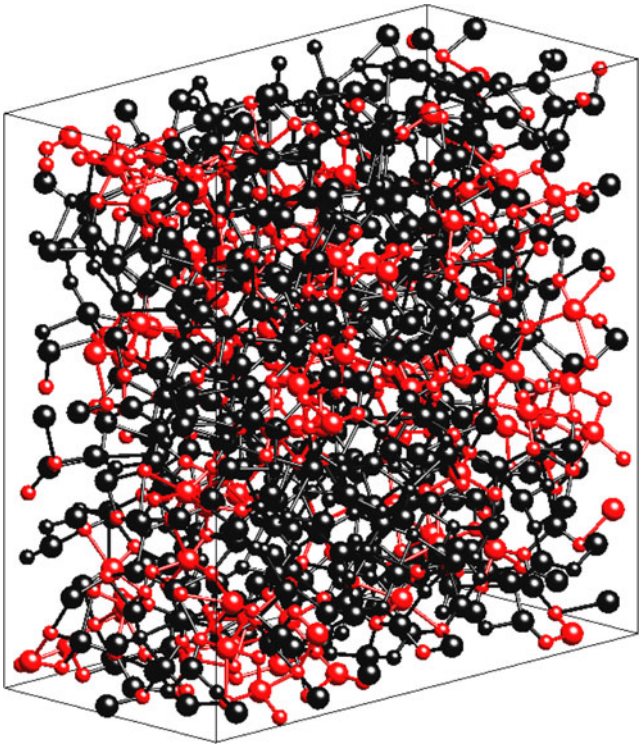

Fig. 14 Distribution of MgO_x coordination units at 3,400 K. The *red regions* are formed by MgO_5 coordination units; The *black regions* are formed by other coordination units. The larger spheres are Mg atoms; the smaller ones represent O atoms (colored online)

4 Conclusions

We have reported a MD study of the microstructure and diffusion in liquid MgO. Our study traces the movement of the MgO_x coordination units ($x=2, 3, 4, 5, 6$) in the network structure of liquid MgO during the simulation time at temperatures ranging from 3,400 to 5,000 K. The results show that each atom goes through a sequence of stages, in each of which it is attached to a fixed MgO_x structure. The lifetime of the coordination unit is strongly temperature dependent and varies from unit to unit. The MSD grows linearly with the number of transitions. The diffusion coefficient in liquid MgO depends on the rate of $MgO_x \rightarrow MgO_{x\pm1}$ transitions and on the ratio $\eta_{sn\text{-}s}=M_{sn}/M_s$ between the number of non-repeated transitions and the number of transitions. Diffusion in liquid MgO occur trough nearest-neighbor atomic exchange among distinct coordination units. As the temperature grows, the transition rate V_{tr} and $\eta_{sn\text{-}s}$ increase. This increases the diffusion coefficient. The distributions of the number of transitions are Gaussians, analysis of which shows that the liquid MgO dynamics is spatially heterogeneous.

Dynamical heterogeneity in liquid MgO is a consequence of structural heterogeneity.

Acknowledgments This research is funded by Vietnam National Foundation for Science and Technology Development (NAFOSTED) under grant number 103.05-2013.30.

References

1. P.K. Dixon, W. Lei, S.R. Nagel, B.D. Williams, J.P. Carini, Scaling in the relaxation of supercooled liquids. Phys. Rev. Lett. **65**(9), 1108–1111 (1990)
2. A. Tolle, H. Schober, J. Wuttke, F. Fujara, Coherent dynamic structure factor of orthoterphenyl around the mode coupling crossover temperature Tc. Phys. Rev. E. **56**(1), 809 (1997)
3. E. Kartini, M.F. Collins, B. Collier et al., Inelastic-neutron-scattering studies on glassy and liquid $Ca_{0.4}K_{0.6}(NO_3)_{1.4}$. Phys. Rev. B **54**(9), 6292 (1996)
4. M.D. Ediger, spatially heterogeneous dynamics in supercooled liquids. Annu. Rev. Phys. Chem. **51**, 99–128 (2000)
5. C.A. Angell, Formation of glasses from liquids and biopolymers. Science **267**(5206), 1924–1935 (1995)
6. D. Chandan, Theoretical approaches to the glass transition in simple liquids. PRAMANA J. Phys. **64**(5), 679–694 (2005)
7. L. Berthier, G. Biroli, Theoretical perspective on the glass transition and amorphous materials. Rev. Mod. Phys. **83**(2), 587–645 (2011)
8. G. Adam, J.H. Gibbs, On the temperature dependence of cooperative relaxation properties in glass-forming liquids. J. Chem. Phys. **43**(1), 139–146 (1965)
9. J.H. Gibbs, E.A. Dimarzio, Nature of the glass transition and the glassy state. J. Chem. Phys. **28**, 373–383 (1958)
10. D. Turnbull, M.H. Cohen, Free-volume model of the amorphous phase: glass transition. J. Chem. Phys. **34**(1), 120–125 (1961)
11. M.H. Cohen, G.S. Grest, Liquid-glass transition, a free-volume approach. Phys. Rev. B **20**(3), 1077–1098 (1979)
12. S. M. Oversteegen, R. Roth, General methods for free-volume theory, 122, 214502 (2005)
13. K.S. Schweizer, Microscopic theory of the dynamics of polymeric liquids: general formulation of a mode-mode-coupling approach. J. Chem. Phys. **91**(9), 5802–5821 (1989)
14. W. GLotze, *In Liquids, Freezing, and Glass Transition*, J.P. Hansen, D. Levesque, J. Zinn-Justin (Eds.) (Elsevier, Amsterdam, 1991), p. 289 (Chapter 5).
15. T. Geszti, Pre-vitrification by viscosity feedback. J. Phys. C Solid State Phys. **16**(30), 5805 (1983)
16. M. Goldstein, Viscous liquids and the glass transition: a potential energy barrier picture. J. Chem. Phys. **51**(9), 3728 (1969)
17. F.H. Stillinger, J.A. Hodgdon, Translation-rotation paradox for diffusion in fragile glass-forming liquids. Phys. Rev. E. **50**(3), 2064–2068 (1994)
18. F.H. Stillinger, J.A. Hodgdon, Reply to "Comment on 'Translation-rotation paradox for diffusion in fragile glass-forming liquids'". Phys. Rev. E. **53**(3), 2995–2997 (1996)
19. F.H. Stillinger, Relaxation and flow mechanisms in 'fragile' glass-forming liquids. j. chem. phys. **89**(10), 6461–6469 (1988)
20. P.G. Debenedetti, F.H. Stillinger, Supercooled liquids and the glass transition. Nature **410**, 259–267 (2001)
21. S. Sastry, The relationship between fragility, configurational entropy and the potential energy landscape of glass-forming liquids. Nature **409**, 164–167 (2001)
22. R.J. Speedy, Relations between a liquid and its glasses. J. Phys. Chem. B **103**(20), 4060–4065 (1999)
23. C.T. Moynihan, C.A. Angell, Bond lattice or excitation model analysis of the configurational entropy of molecular liquids. J. Non-Cryst. Solids **274**(1), 131–138 (2000)
24. S. Sastry, Evaluation of the configurational entropy of a model liquid from computer simulations. J. Phys. Condens. Matter **12**(29), 6515 (2000)
25. H. Sillescu, Heterogeneity at the glass transition: a review. J. Non-Cryst. Solids **243**(2), 81–108 (1999)
26. S.C. Glotzer, Spatially heterogeneous dynamics in liquids: insights from simulation. J. Non-Cryst. Solids **274**(1), 342–355 (2000)
27. R. Bohmer, Nanoscale heterogeneity of glass-forming liquids: experimental advances. Curr. Opin. Solid State Mater. Sci. **3**, 378–385 (1998)
28. R. Richert, Heterogeneous dynamics in liquids: fluctuations in space and time. J. Phys. Condens. Matter **14**(23), R703 (2002)
29. E.R. Weeks, J.C. Crocker, A.C. Levitt et al., Three-dimensional direct imaging of structural relaxation near the colloidal glass transition. Science **287**(5453), 627 (2000)
30. N. Vang Hong, M.T. Lan, P.K. Hung, Structure and dynamics of liquid MgO under high pressure. Int. J. High Press. Res. **32**(4), 509–523 (2012)
31. S. Xiaowei, C. Qifeng, C. Yandong, W. Chengwei, Properties of MgO at high pressures: shell-model molecular dynamics simulation. Physica B **370**, 186–194 (2005)
32. P. Tangney, S. Scandolo, Melting slope of MgO from molecular dynamics and density functional theory. J. Chem. Phys. **131**, 124510 (2009)
33. B. Bijaya, Karki, Dipesh Bhattarai, and Lars Stixrude, first-principles calculations of the structural, dynamical, and electronic properties of liquid MgO. Phys. Rev. B **73**(174208), 1–7 (2006)
34. A. Aguado, P.A. Madden, New insights into the melting behavior of mgo from molecular dynamics simulations: the importance of premelting effects. Phys. Rev. Lett. **94**, 68501 (2005)
35. N.P. de Koker, L. Stixrude, B.B. Karki, Thermodynamics, structure, dynamics, and freezing of Mg2SiO4 liquid at high pressure. Geochim. Cosmochim. Acta **72**, 1427–1441 (2009)
36. F.J. Spera, M.S. Ghiorso, D. Nevins, Structure, thermodynamic and transport properties of liquid MgSiO3: comparison of molecular models and laboratory results. Geochim. Cosmochim. Acta **72**, 1427–1441 (2009)
37. L. Cormier, G.J. Cuello, Mg coordination in a $MgSiO_3$ glass using neutron diffraction coupled with isotopic substitution. Phys. Rev. B **83**, 224204 (2011)
38. S. Kohara, K. Suzuya, K. Takeuchi, C.K. Loong, M. Grimsditch, J.K.R. Weber, J.A. Tangeman, T.S. Key, Glass formation at the limit of insufficient network formers. Science **303**, 1649–1652 (2004)
39. G. Omar Adjaoud, Steinle-Neumann, Sandro Jahn, Mg_2SiO_4 liquid under high pressure from molecular dynamics. Chem. Geol. **256**, 185–192 (2008)